





Article

# Natural Versus Anthropic Influence on North Adriatic Coast Detected by Geochemical Analyses

Eliana Barra <sup>1,2</sup>, Francesco Riminucci <sup>1,3,\*</sup> , Enrico Dinelli <sup>2</sup> , Sonia Albertazzi <sup>1</sup>,  
Patrizia Giordano <sup>4</sup>, Mariangela Ravaioli <sup>1</sup>  and Lucilla Capotondi <sup>1,\*</sup> 

<sup>1</sup> Istituto di Scienze Marine-Consiglio Nazionale delle Ricerche ISMAR-CNR, Via P. Gobetti 101, 40129 Bologna, Italy; eliana.barra@studio.unibo.it (E.B.); sonia.albertazzi@bo.ismar.cnr.it (S.A.); mariangela.ravaioli@bo.ismar.cnr.it (M.R.)

<sup>2</sup> BiGeA-Dipartimento di Scienze Biologiche, Geologiche e Ambientali, Università di Bologna, Via Zamboni 33, 40126 Bologna, Italy; enrico.dinelli@unibo.it

<sup>3</sup> Consorzio Proambiente S.c.r.l., Tecnopolo Bologna CNR, Via Gobetti 101, 40129 Bologna, Italy

<sup>4</sup> Istituto di Scienze Polari-Consiglio Nazionale delle Ricerche ISP-CNR, Via P. Gobetti 101, 40129 Bologna, Italy; patrizia.giordano@cnr.it

\* Correspondence: francesco.riminucci@bo.ismar.cnr.it (F.R.); lucilla.capotondi@bo.ismar.cnr.it (L.C.)

Received: 28 July 2020; Accepted: 15 September 2020; Published: 21 September 2020



**Abstract:** This study focused on the geochemical and sedimentological characterization of recent sediments from two marine sites (S1 and E1) located in the North Adriatic Sea, between the Po River prodelta and the Rimini coast. Major and trace metal concentrations reflect the drainage area of the Po River and its tributaries, considered one of the most polluted areas in Europe. Sediment geochemistry of the two investigated sites denote distinct catchment areas. High values of Cr, Ni, Pb and Zn detected in sediments collected in the Po River prodelta (S1 site) suggest the Po River supply, while lower levels of these elements characterize sediments collected in front of the Rimini coast (E1 site), an indication of Northern Apennines provenance. Historical trends of Pb and Zn reconstructed from the sedimentary record around the E1 site document several changes that can be correlated with the industrialization subsequent to World War II, the implementation of the environmental policy in 1976 and the effects of the Comacchio dumping at the end of 1980. At the S1 site, the down core distributions of trace elements indicate a reduction of contaminants due to the introduction of the Italian Law 319/76 and the implementation of anti-pollution policies on automotive Pb (unleaded fuels) in the second half of the 1980s.

**Keywords:** northern Adriatic Sea; anthropic signal; trace metals concentration; marine sediments

## 1. Introduction

Sedimentary deposits represent an important natural archive of environmental change. Their study allows the evaluation of the extent and the effect of anthropogenic inputs [1]. Indeed, marine sediments act as sinks and sources of contaminants delivered to the sea from inland activities. Therefore, the knowledge of the type and concentration of contaminants, along with their spatial distribution, pathways and historical trends are essential for supporting measures to mitigate future impacts on marine ecosystems. Hence, an exhaustive assessment of the natural geochemical background is mandatory, when dealing with inorganic contaminants [2].

The Po River plain is one of the most industrialized and agriculturally developed areas in Europe, generating nearly 40% of the Italian Gross Domestic Product. The high concentration of industrial, zootechnical and agricultural activities critically intensifies the risk of heavy-metal contamination of the prodelta area, coastal lagoons [3–6] and in the neighboring marine environments [7,8].

To evaluate the anthropic effects on coastal environments, we report integrated geochemical and sedimentological analyses performed on marine sediment cores collected in the North Adriatic at the Po River delta and the Rimini coast (Figure 1). In this study, we aimed: (1) to provide additional information about the geochemical composition and distribution of the surface marine sediments, including major and trace element concentrations; and (2) to investigate the recent (the last 100 years) anthropic influence on the *Emilia-Romagna* coast.

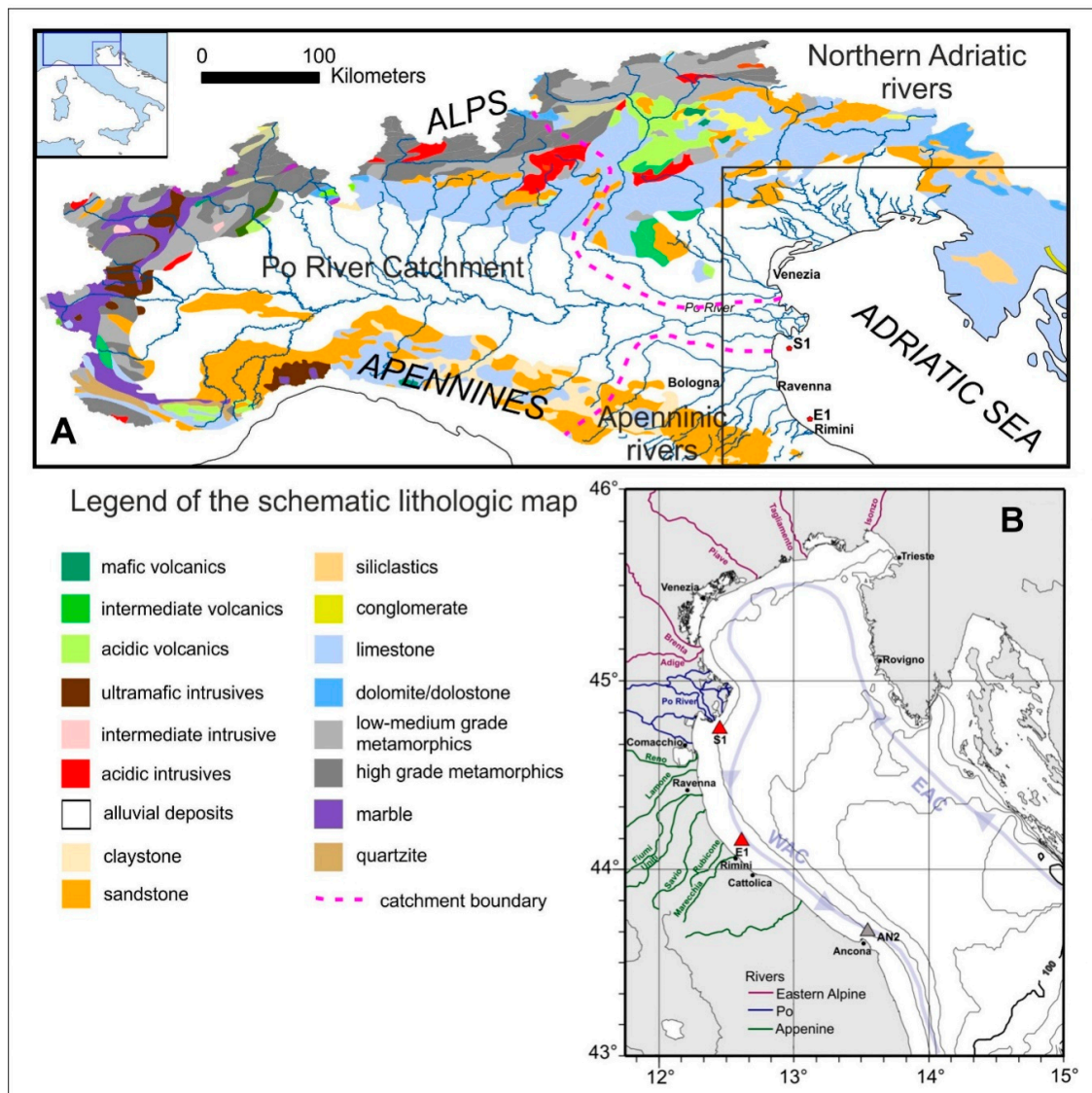


**Figure 1.** (A) Lithologic map of the Po River drainage basin (data from 1:1 Million Surface Geology—European Geological Data Infrastructure: <https://egdi-v6.geology.cz/?ak=detailall&uuid=5729ffdf-2558-48fc-a5d2-645a0a010855>). Major Po contributor rivers are also indicated. (B) Schematic surface circulation pattern of the Northern Adriatic Sea. EAC: Eastern Adriatic Current; WAC: Western Adriatic Current [9]. Triangles represent S1, E1 (this work, red triangles) and AN2 (grey triangle) [10] coring sites.

### Study Area

The North Adriatic Sea (NAS) is an epicontinental basin characterized by a global cyclonic circulation with seawater inflow to the northwest along the Croatian coast (EAC) and outflow to the southeast along the Italian coast (WAC) [9] (Figure 1). This general pattern is greatly influenced by winds, mainly Bora and Scirocco [11,12], and by lateral freshwater inputs [13]. Freshwater runoff enters the NAS from eastern Alpine and northern Apennine rivers located mainly along the

Italian coastline. The largest source of freshwater and sediments is represented by the Po River (mean annual discharge of  $1500 \text{ m}^3 \text{ s}^{-1}$ ) [14–16]. The Po River catchment extends from the Central and Western Alps up to the northwestern Apennines and includes more than 140 Alpine and Apennine tributaries that discharge water and sediment into the Po River [17] (Figure 1). The hydrologic behavior of the Po River is characterized by the mixed Alpine/Apennine discharge regime resulting in two flooding periods in late fall and spring, due to intense precipitation and snow melting, respectively [18].

Sediment accumulation rates range 1.2–30 mm/year with the highest value recorded in the study area, and then accumulation rates decrease southward and toward the open sea [15]. Several studies [18–21] pointed out a decrease of the sediment supply in terms of both suspended and bed loads, from the Po and the Northern Apennines rivers, after 1945. An additional decrease was observed in the 1980s when the *Emilia-Romagna* region underwent heavy urbanization of both coastal and inland areas, as well as other parts of the Po River plain [18,19,22,23]. The Apennine rivers—which flow into the NAS encompassing the area between Ravenna and Rimini (Reno, Lamone, Bevano, Fiumi Uniti, Savio, Rubicone, Uso and Marecchia)—are characterized by smaller catchments areas. Their courses are almost straight, and their flow rate is subject to the rainfall regime resulting in very low discharges in summer, when hydric demand and evapotranspiration are the highest [20,24,25].

Geochemical characterization of Po Plain late Quaternary deposits [17,26–31] document that they preserve fingerprints of the related catchment basins. In detail, nickel and chromium have been used as tracers of sediment provenance since Cr-rich (and Ni-rich) sediments have been found to be representative of the Po River drainage basin, whereas sediments with lower Cr and Ni values have been related to the Apennines supply [26,28]. Their concentration is due to the contribution of ultramafic rocks in the Po River catchment (Figure 1). Although Cr and Ni could also be affected by anthropogenic sources, they seem to be minor, since comparable results were reported for present day Po River sediments and Holocene marine deposits in the area [27].

## 2. Materials and Methods

### 2.1. Sampling and Analyses

We investigated the marine area around two fixed observatories (the E1 meteo-oceanographic buoy and the S1-GB dynamic pylon [32,33]), part of the Italian LTER network (long-term ecological research network, <https://deims.org/6869436a-80f4-4c6d-954b-a730b348d7ce>) deployed to study the ecosystems and the long-term response to environmental, societal and economic drivers [34]. Six sediment cores were collected with a box-corer in 2014, 2016 and 2017 during the oceanographic cruises EL-14, LTER-ANOC16 and INTERNOS17 onboard the R/V Dallaporta (Table 1).

**Table 1.** Details of sampling stations.

Cores	Latitude	Longitude	Site	Water Depth (m)	Core Length (cm)
S1-EL14	44.737° N	12.447° E	S1	21	17
E1-EL14	44.141° N	12.573° E	E1	10.5	15
S1-ANOC16	44.742° N	12.452° E	S1	21	17.5
E1-ANOC16	44.148° N	12.577° E	E1	10.5	16
S1-INT17	44.742° N	12.459° E	S1	21	18
E1-INT17	44.143° N	12.572° E	E1	10.5	10.5

Core locations and study areas, namely S1 (*Delta del Po*) and E1 (*Costa Romagnola*) (summarized above as S1 and E1, respectively), are shown in Figure 1. Each box-core was subsampled with smaller PVC cores (diameter 8 cm) and stored at 4 °C [35,36] directly on the vessel. At the ISMAR-CNR laboratories, each core was described and subsampled at 1 or 2 cm of thickness. The samples were dried at 60 °C and the porosity was calculated assuming a sediment density of  $2.55 \text{ g cm}^{-3}$  [37]. Dried sediment levels from all six cores were slightly disaggregated and analyzed for the radiotracer  $^{137}\text{Cs}$ , by non-destructive gamma-ray spectrometry using two intrinsic Ge detectors.

Sediment samples were put into cylindrical transparent plastic jars, pressed and counted for 24 h. Activities were measured following Albertazzi et al. [38] and Frignani et al. [39]. Both detectors were connected to an integrated gamma-spectrometry system, the *DSPEC-Ortec*. Output spectra were processed and calibrated by using the *Gammavision-Ortec* software. All concentrations and activities are relative to dry weight and are expressed in  $\text{Bq kg}^{-1}$ . Detector efficiency was estimated using samples of sediment spiked with multipeak standard solutions (QCY58) counted in standard geometry jars (5–10–15–20 ml). Accuracy was checked periodically by using certified reference sediments (IAEA-TEL-2012-03).

To assess grain-size distributions, the organic content was firstly removed by treating the samples with  $\text{H}_2\text{O}_2$ ; subsequently, sediments were wet sieved with a 63- $\mu\text{m}$ -net size to separate coarse- and fine-grained fractions. Finally, the coarse fraction was analyzed using a stack of ASTM sieves, while the finer sediments by an X-ray sedigraph *Micromeritics 5120*, in order to quantify the silt and clay fractions. Results are relative to dry weight and are expressed as percentages of grain-size fractions. Sediments were also analyzed for geochemical composition at the BiGeA laboratories, by means of X-ray fluorescence spectrometry. At least 3 g of each dried sediment layer were ground in an agate mortar and then pressed with 7 g of  $\text{H}_3\text{BO}_3$  to obtain powder pellets. Geochemical analyses were carried out by using a *Panalytical Axios 4000* X-ray spectrometer, to quantify major (Si, Ti, Al, Fe, Mn, Mg, Na, K and P) and trace element (Sc, V, Cr, Co, Ni, Cu, Zn, Ga, As, Rb, Sr, Y, Zr, Nb, Ba, La, Ce, Pb, Th, S, Ba and Mo) contents, expressed as dry weight percentages (dw %) and in  $\text{mg kg}^{-1}$ , respectively (Appendix A). In this work, the trace metal concentrations are normalized to  $\text{Al}_2\text{O}_3$ , one of the most commonly used normalizers in sediment studies [40]. For a more detailed description of the historical trend of anthropic influence at the S1 site, the results for Zn and Pb were integrated with the literature data (see Section 4.3).

The Loss On Ignition (LOI), which includes contribution from organic matter, crystalline water and carbonates, was estimated in terms of weight loss after heating at 950 °C to constant weight.

## 2.2. Background Levels

To evaluate the anthropogenic signals in S1 and E1 sites, we compared the data with the background trace metal values. As work strategy, for the S1 site, we considered as background values from adjacent areas available from the literature [10,41,42] (Table 2), and, for the E1 site, we chose the mean values detected in the 1900–1920 interval (Table 2 and interval 12–15 cm in Figure 5) as representative of the pre-industrial values.

**Table 2.** Mean and standard deviation of trace metals in S1 and E1 sediment cores (ANOC-2016) and background (Bkg) levels.

	Zn	Pb	Cu	Cr	Ni
S1-Mean	129 ± 8	36 ± 3	34 ± 3	183 ± 4	128 ± 3
S1-Bkg *	84	14	30	152	61
E1-Mean	79 ± 7	22 ± 4	18 ± 3	139 ± 4	80 ± 7
E1-Bkg	80	20	16	142	91

Metal concentrations are reported in  $\text{mg kg}^{-1}$ . \* Data from literature [10].

## 3. Results

### 3.1. Porosity

Porosity vertical profiles of S1 sediment cores do not show evident variations (values around 0.65–0.69, Figure 2). A slight decrease of porosity is detected only in the bottom layer documenting an increase of sediment compaction. On the other hand, the E1 sedimentary interval displays a larger variability of porosity (ranging from 0.50 to 0.69, Figure 2). The higher values are recorded in the

first 4 cm with a clear decreasing trend and with the downward porosity stabilizing toward the lower values (Figure 2).

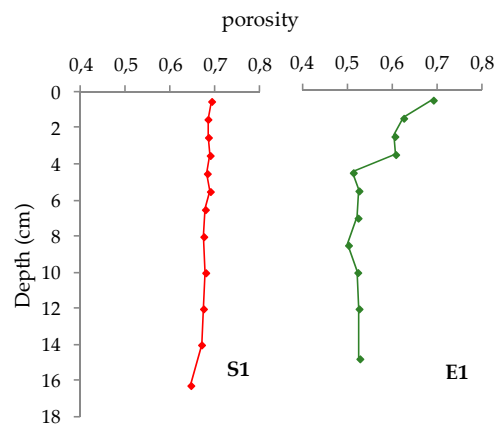


Figure 2. Porosity vs. depth profiles for S1 and E1 cores (cruise ANOC-16).

### 3.2. <sup>137</sup>Cs Activity

Sedimentation rates were estimated using the vertical distribution of <sup>137</sup>Cs activity [43]. In the S1 investigated cores, results point out a <sup>137</sup>Cs activity range of  $10.22 \pm 1.55$  to  $29.01 \pm 4.15$  Bq kg<sup>-1</sup> with a median value of 17.74 Bq kg<sup>-1</sup> (Figure 3a–c). The trends are very similar, and the highest value are detected in the S1-INT17 core at 2 cm of depth (Figure 3c). Cores from E1 (Figure 3d–f) display very low <sup>137</sup>Cs activity, between  $3.28 \pm 2.1$  and  $6.45 \pm 2.78$  Bq kg<sup>-1</sup> with a median value of 5.39 Bq kg<sup>-1</sup>.

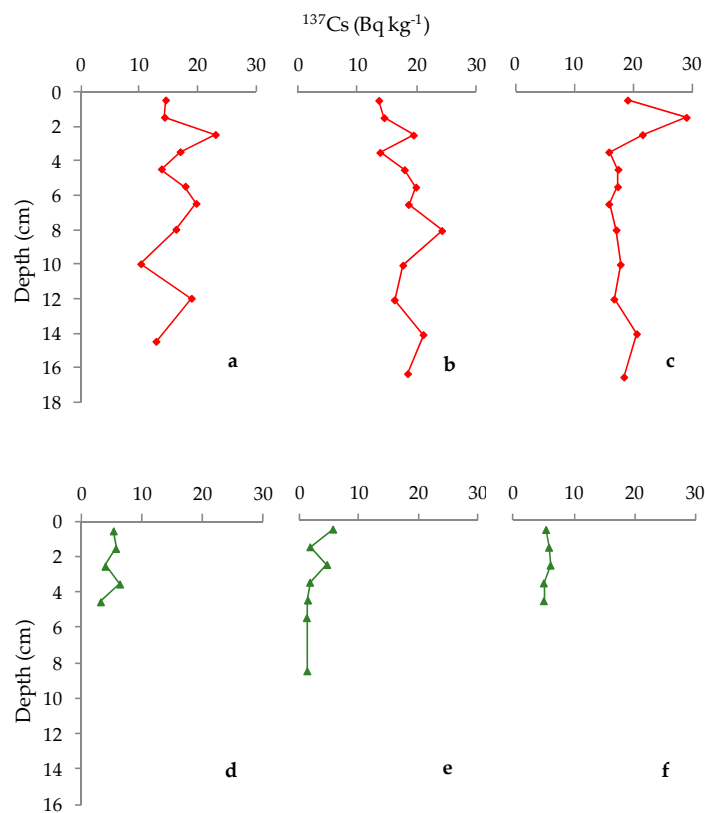
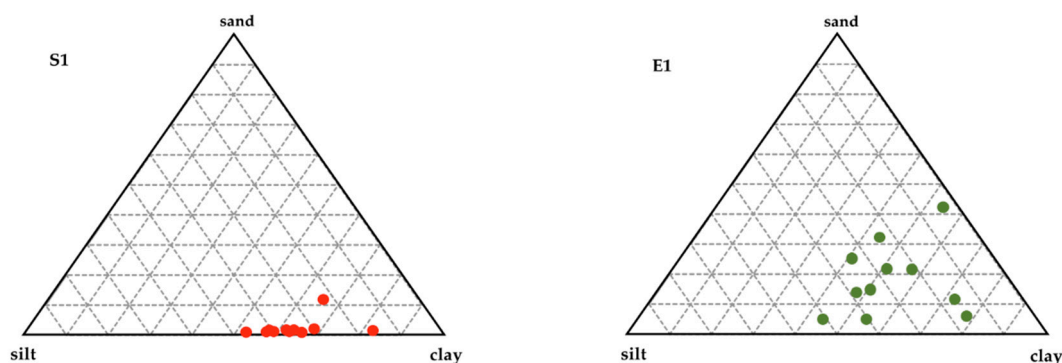


Figure 3. Depth profiles of <sup>137</sup>Cs for: (a) S1-EL14; (b) S1-ANOC16; (c) S1-INT17; (d) E1-EL14; (e) E1-ANOC16; and (f) E1-INT17.



### 3.3. Grain Size

Grain size results are reported in Figure 4. The S1 sediments are composed prevalently by clay and silt fractions (around the 90%) in almost all levels, in line with the literature data [44,45]. The E1 sediments are characterized by a more heterogeneous composition; they consist of silty clays with high sand percentages (40%) in the surficial levels (Figure 4).



**Figure 4.** Shepard diagram of the sediment composition in S1 and E1 (cruise ANOC-16) sediment cores.

### 3.4. Geochemistry

The chemical composition of sediments collected at the S1 and E1 sites is reported in Table 3 (complete geochemical dataset in Appendix A). High MgO content characterizes sediments from the S1 site, whereas higher CaO content is observed in sediments from E1. Regarding trace elements, sediments from the S1 area have higher concentrations of Cr, Cu, Ni, Pb and Zn than those from the E1 site.

**Table 3.** Geochemical analyses of S1 and E1 sediment cores (ANOC-16).

Major Elements (dw %)				
	S1		E1	
	Min–max	Mean	Min–max	Mean
Al <sub>2</sub> O <sub>3</sub>	13.36–13.94	13.64 ± 0.17	11.90–14.81	12.93 ± 0.89
MgO	3.98–4.75	4.45 ± 0.20	3.49–3.85	3.72 ± 0.13
CaO	8.77–9.79	9.49 ± 0.30	9.67–12.73	11.34 ± 0.90
Trace elements (mg kg <sup>-1</sup> )				
	S1		E1	
	Min–max	Mean	Min–max	Mean
Cr	176–190	183 ± 4	132–146	139 ± 4
Cu	28–40	34 ± 3	15–23	18 ± 3
Ni	120–128	128 ± 3	71–95	80 ± 7
Pb	32–39	36 ± 3	18–29	22 ± 4
Zn	114–138	129 ± 8	71–92	79 ± 7

Major elements are reported in percent dry weight. Trace elements are reported in mg kg<sup>-1</sup>. Min, max, mean and standard deviation values of all sediment layers.

Geochemical analyses show that Pb and Zn average concentrations of the S1 sediment core are, respectively, 1.5 and 0.5 times higher than the background levels of the site (Table 2), while the E1 average concentrations and the background values are similar.

Depth profiles of cores from the S1 site show an increasing trend of the MgO contents upwards, relatively stationary concentrations of Cr and Ni and gradual decreasing upward trend of Pb (from 39 to 33 mg kg<sup>-1</sup>), whereas Zn shows a slight increase between –16 and –8 cm (from 132 to 138 mg kg<sup>-1</sup>) and then a decrease to 114 mg kg<sup>-1</sup> Zn at the top (Figure 5). In cores from E1 site, MgO and Ni contents are relatively uniform, Cr reaches a peak at ~5 cm of 146 mg kg<sup>-1</sup> and Zn and Pb contents show a

moderate decreasing trend between 16 and 7 cm, a sharp increase between 7 and 2 cm and peaks at ~3 cm reaching 91 and 29 mg kg<sup>-1</sup>, respectively.

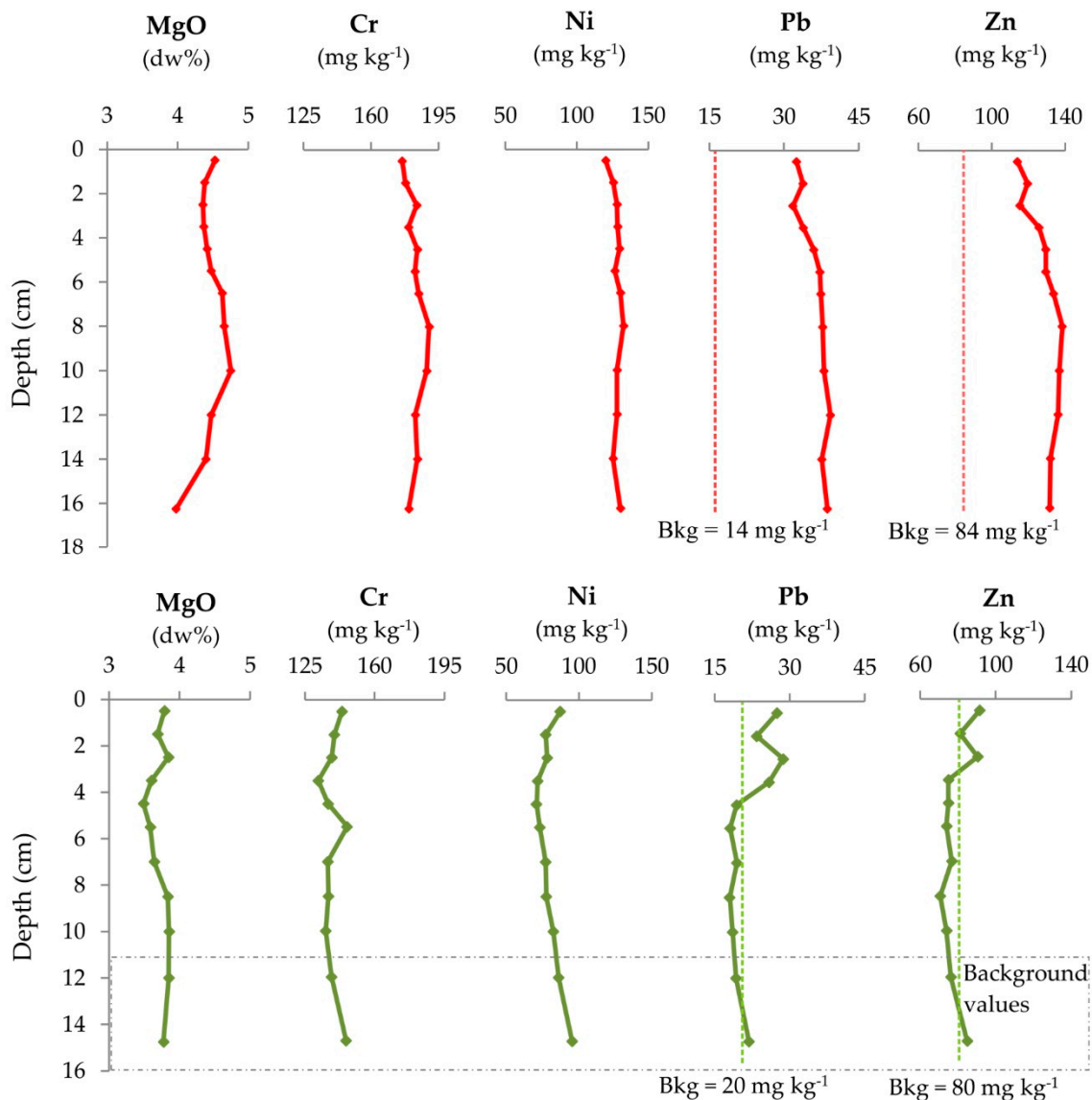


**Figure 5.** Depth profiles of selected major (MgO) and trace elements (Cr, Ni, Pb and Zn) in S1 (red line) and E1 (green line) sediment cores (ANOC-16).

#### 4. Discussion

##### 4.1. Dating

Activity profiles of <sup>137</sup>Cs in the sediment cores were used to estimate the Sediment Accumulation Rates (SAR) of the two investigated areas. Unfortunately, the short time interval recorded by our samples (max 18 cm, Table 1) due to the local high accumulation rate at the S1 site [15] did not allow us to identify the <sup>137</sup>Cs reference peak corresponding to the 1986 Chernobyl fallout (Figure 3). Consequently, for this area, we used the most recent available value of 19.4 mm/year [15,46]. Instead, we related the highest value in the <sup>137</sup>Cs distribution, detected at 3.5 cm in the E1 cores (EL14 core, Figure 3) to the 1986 event estimating a SAR of 1.2 mm/year for this site, a value comparable with those from the literature [15,38,43,47]. These results indicate that the stratigraphic succession sampled in S1 represents approximately nine years of history, while the sedimentary record recovered in E1 extends to the early 1900s (Figure 7).

#### 4.2. Geochemical Signature of Marine Sediments

As reported in several studies [17,48–50], Cr, Ni and Mg concentrations can be used to discriminate the source areas of sediments. We compared Cr, Ni and Mg contents in the sediments from the S1 and E1 sites with those from the literature. In detail, we considered the geochemistry of deposits from the Po and Apennines rivers [30] and from boreholes in the inland areas [27].

The comparison shows that the concentrations of Cr and Ni in sediments from the Po River delta (S1 site) are very similar to those detected in sediments recovered along the Po River [30], suggesting for this area a prevailing to exclusive sediments supply from the Po River (Figure 6a). On the contrary, Cr and Ni concentrations measured in sediments from the E1 site show a wider dispersion with values comparable to those of the Northern Apennines rivers (Reno, Lamone, Fiumi Uniti, Bevano, Savio Rubicone, Uso and Marecchia), indicating an Apenninic sedimentary source for this area. These different sources of sedimentary material are in agreement with previous investigations [17,27]. It is noteworthy that the Cr and Ni concentrations of S1 site exceed the maximum permissible concentrations, according to the Italian environmental legislation, for unpolluted sites [51] (Table 4). These have a natural origin, derived from the outcrops of ultramafic rocks in the Western Alps and in the Northern Apennines, as documented by previous studies on both river and marine sediments [8,30,49].

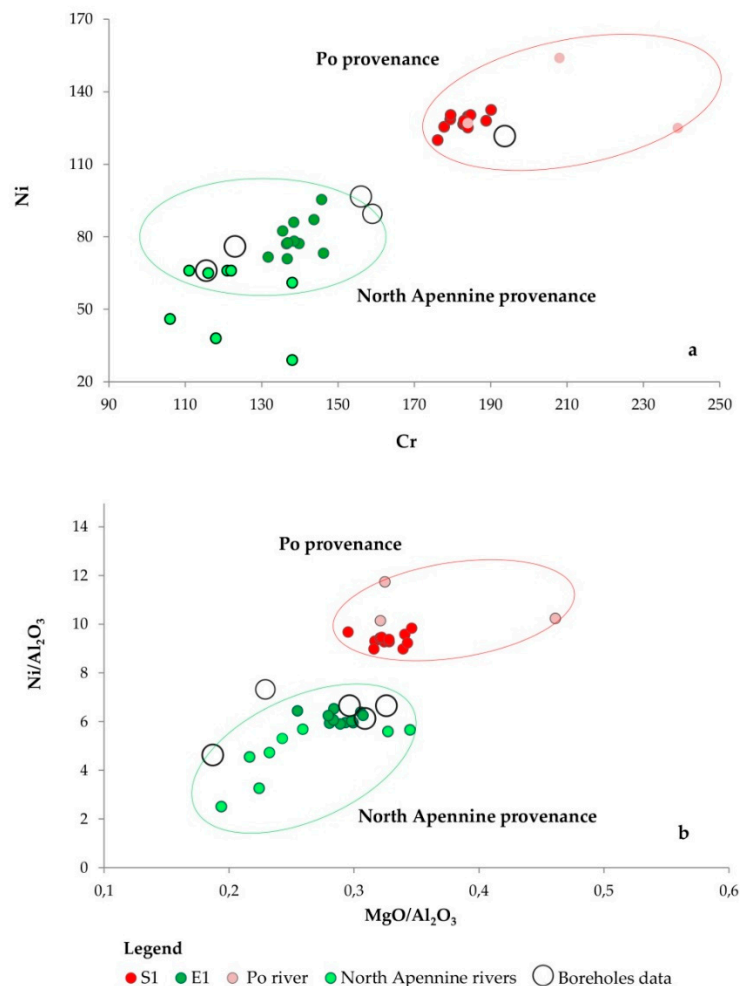


**Figure 6.** (a) Binary plots of Ni vs. Cr and (b) Ni/Al<sub>2</sub>O<sub>3</sub> vs. MgO/Al<sub>2</sub>O<sub>3</sub> ratios. Our samples are indicated as green and red dots. Reference data for rivers (light green, Apennines; light red, Po River) derive from tables presented in [30]. Reference data for boreholes (empty big circles) represent the average values presented in [27]. Provenances fields (green and red circles) are drawn in accordance with literature data [17,26–28,50,51].



**Table 4.** Mean metal concentrations (this work).

<b>S1</b>	<b>Cr</b>	<b>Ni</b>	<b>Pb</b>	<b>Zn</b>
mean	183	128	36	129
min	179	120	32	114
max	190	133	39	138
<b>E1</b>				
mean	139	80	22	79
min	132	71	18	71
max	149	95	29	92
<b>Csc D.lgs 152/2006 *</b>	150	120	100	150
<b>LCB **</b>	100	70	40	100
<b>LCL **</b>	360	75	70	170

\* Italian Sediment Quality benchmarks, \*\* APAT and ICRAM [52]. The LCB represent the mean values of chemical content in the Italian marine sediments, whereas LCL refers to the highest values in Italian marine sediments. Values are in mg kg<sup>-1</sup>.

In addition, Ni and Mg concentrations also highlight different input sources for our samples (Figure 6b). The Po River is the main source of Cr and Ni for the Adriatic Sea, accounting for ~50% of total Cr and Ni fluvial inputs [8]. According to a recent study [17], Ni/Al<sub>2</sub>O<sub>3</sub> and MgO/Al<sub>2</sub>O<sub>3</sub> ratios close to 6 and 0.3 mg kg<sup>-1</sup>, respectively, reflect an Apennine signature of the E1 samples, whereas values of 10 and 0.32 mg kg<sup>-1</sup> document the Po River provenance for the S1 samples (Figure 6b). Samples collected in the 1980s [53] were characterized by a southward decrease in magnesium rates in the northern-central Adriatic Sea, which is probably due to a higher content of dolomite (rich in Mg) brought by the Po and Alpine rivers. Based on the observations reported by Amorosi et al. [28], a value of Cr/Al<sub>2</sub>O<sub>3</sub> ratio > 11.5 can be considered a clear signal of the sediment provenance dominated by the Po River supply. These data are consistent with the relatively high Cr concentrations detected in S1 sediments (Table 3 and Figures 5 and 7). The upward increasing trend of Cr/Al<sub>2</sub>O<sub>3</sub> in the E1 depth profile (Figure 7) may be interpreted as a gradual increase of the Po River contribution in the E1 site over the years, in particular after the 1940s. This trend seems in contrast with the decrease of sediment supply by the Po River recorded after 1945 (with a generalized phase of degradation and partial retreat of the entire Po River delta) caused by the construction of a dam [21,54], riverbed mining activities and the channelization of watercourses [55]. The most significant retreat phase, with rates in the order of tens of meters per year, reached its peak between 1954 and 1978 [56] when the E1 core recorded the highest Cr/Al<sub>2</sub>O<sub>3</sub> ratio (Figure 7). The reduction in sediment supply, combined with the recent increase in storm events produced an increase of coastal erosion in the area [18–20,57]. Sediment transport is enhanced in the northern Adriatic by the northeasterly Bora wind that intensifies waves and currents, especially in winter, with an average southward transport along the shelf and little across-shelf transport [58]. The Cr increase in the surficial sediments was recorded not only in the E1 site, but also further south, in the AN2 core offshore Ancona (Figure 1) [10]. We speculate that the high Cr values of sediments from the stations south of the Po River prodelta result from the southerly deposition of the eroded sediments of the delta wedge.

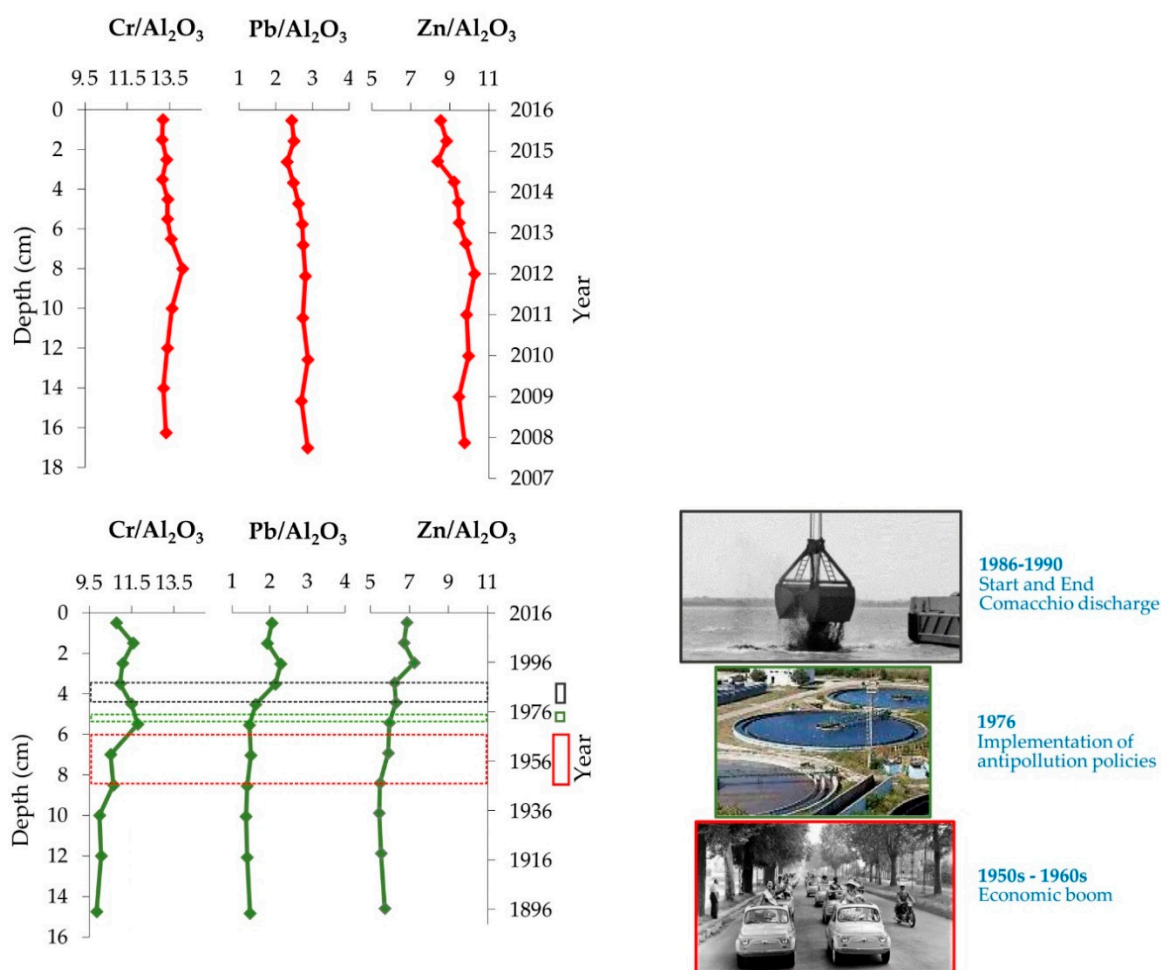


**Figure 7.** Down-core variability of geochemical proxies ( $Pb/Al_2O_3$  and  $Zn/Al_2O_3$ ) in S1 (red line) and E1 (green line) measured in ANOC16 cores.

### 4.3. Anthropogenic Signal

The Zn and Pb concentrations found in well dated sediment cores collected at several locations along the western Adriatic Sea were successfully used to reconstruct the anthropogenic influence in the past [7,8,10].

In samples from S1 site, Zn and Pb values fall far beyond the Holocene reference field, corresponding to the pre-industrial concentrations [10,41,42] (Table 2). The investigate time interval is limited (only the last nine years), however it is interesting to evidence that the observed decline over recent time of Pb and Zn concentrations (Figure 7) is in line with the historical trend reconstructed using data reported in the literature [59,60] (Table 5 and Appendix B) in the same area. Perhaps this is the result of the application of the Merli Italian Law 319, adopted in 1976, that regulates the concentrations of contaminants in wastewaters for environmental protection. The same assumption was suggested to explain the low content of trace metals observed in the sediments from the River Po delta [10]. Additionally, the Pb content reduction may be in response to the implementation of anti-pollution policies on automotive Pb in the second half of the 1980s in Western Europe [61].

At the E1 site, the longer time interval sampled (see Section 4.1) provides the history of contamination during the last 100 years. The E1 normalized depth profiles of Pb and Zn (Figure 7) display a gradual increasing accumulation trend from the 1940s with a peak from 1980 to 2000 in particular for Pb concentration.

**Table 5.** Trace metals concentration detected in the S1 area over the time (data from this work and from literature).

Year	Zn	Pb	References
2016	114	33	This work
2007	132	39	This work
1996	162	44.7	Ianni et al., 2000 [59] (site 103)
1977	189	68.3	Frasconi et al., 1984 [60] (site 30)

Values are reported in  $\text{mg kg}^{-1}$  and not normalized to  $\text{Al}_2\text{O}_3$  in order to perform the comparison between different datasets.

The detected major presence of these elements in the area around the mid-1940s is probably related to the gradual industrialization of the region after World War II. It is worth noting that, in Italy, the time interval of 1945–1963, known as “Economic Miracle”, experienced a strong industrial development with an increase of the mechanical, chemical and ceramics industries [7].

The observed increase in trace metals is consistent with what was found in previous investigations carried out along the coast between Cattolica and the mouth of the Rubicone River [62]. The strong increase from the 1980s (Figure 7, E1 site) correlates in time with marine dumping off Comacchio from 1986 to 1990, used as the disposal sites for dredged materials from the Ravenna port [7,63]. In our opinion, the dumping influenced directly or indirectly the surrounding environment since the activity can destroy and/or degrade habitats for species as well as cause coastal pollution. The documented high accumulation of Pb and Zn may be explained with the southward dispersion of contaminated sediments under the influence of the WAC (Figure 1) from the dumping site to the E1 site located approximately 60 nautical miles away. The recent decrease of Zn and Pb observed since the early 2000s may be related to the application of the Italian Law 319/76 as mentioned above for S1 site.

## 5. Conclusions

Geochemical and distribution analyses of trace elements were performed on the marine sediments from two sites (E1 and S1) located along the western Adriatic coast.

The concentration of some main and trace elements (MgO, Cr and Ni) compared with the literature data allowed us to highlight that the S1 sediments composition largely reflects the discharges of the Po River, whereas sedimentation at the E1 site results mostly controlled by the supplies from the northern Apennines rivers, with only a marginal contribution from the Po River system. The results confirm the presence of high concentrations of Cr and Ni related to the discharge of the Po River and due to the natural presence of ultramafic rocks in its drainage basin. The high Cr values observed in the sediments of E1 station, at the south of the Po prodelta, indicate a southern deposition of the recently eroded sediments of the delta wedge. The accumulation values of trace metals in the two sites show a significant decrease over time, especially near the prodelta sediments of the Po River. Finally, using the elements Pb and Zn as diagnostic of anthropogenic impact, we reconstructed the historical trends of pollution sources. In particular, the results of the E1 site highlight the impact due to the increase in the industry after World War II, the implementation of environmental policy in 1976 and the presence of the Comacchio dumping at the end of 1980.

**Author Contributions:** E.B. wrote the preliminary draft of the manuscript with the support of the other authors; samples collection, analysis and data validation were carried out by S.A., E.D., F.R., P.G., L.C. and M.R.; S.A. and F.R. edited the figures; all authors discussed the results and contributed to the manuscript; L.C. and F.R. revised the final version; and M.R. was the P.I. of the scientific project and provided financial support for the publication. All authors have read and agreed to the published version of the manuscript.

**Funding:** This work was supported by the Jerico-NEXT project (H2020-INFRAIA-2014-2015 Research and Innovation action) and RITMARE Italy Flagship Project (SP5-WP3). The research is part of the LTER Network (<https://deims.org/6869436a-80f4-4c6d-954b-a730b348d7ce>) (Sites S1-GB and E1). This is contribution No. 2032 of the of the Marine Science Institute Consiglio Nazionale delle Ricerche, Bologna.

**Acknowledgments:** This article is in memory of Giovanni Bortoluzzi, a friend and colleague who dedicated his work to the development and support of marine observatories. We are very grateful to the technical staff of DALLAPORTA research vessel and to Mauro Bastianini cruise leader of the LTER-ANOC16, INTERNOS17 oceanographic cruises. We thank the CNR DCSR—Ufficio Programmazione e Grant Office for the technical and logistical support. We also thank Andrea Gallerani and Valerio Funari for their help in preparing the samples for analysis and Michael Marani and Marco Ligi for the helpful suggestions.

**Conflicts of Interest:** The authors declare no conflict of interest. The funders had no role in the design of the study, in collection, analyses, or interpretation of the data; in the writing of the manuscript, or in the decision to publish the results.

## Appendix A

**Table A1.** Geochemical data from LTER-ANOC16 cores.

Major elements (dw %)				
		S1		E1
	Min-max	Mean	Min-max	Mean
SiO <sub>2</sub>	40.21–42.82	41.64 ± 0.88	41.81–45.24	43.63 ± 0.92
TiO <sub>2</sub>	0.61–0.64	0.62 ± 0.01	0.58–0.67	0.62 ± 0.03
Al <sub>2</sub> O <sub>3</sub>	13.36–13.94	13.64 ± 0.17	11.90–14.81	12.93 ± 0.89
Fe <sub>2</sub> O <sub>3</sub>	5.83–6.21	6.01 ± 0.13	4.91–6.43	5.48 ± 0.45
MnO	0.10–0.13	0.11 ± 0.01	0.10–0.12	0.11 ± 0.01
MgO	3.98–4.75	4.45 ± 0.20	3.49–3.85	3.72 ± 0.13
CaO	8.77–9.79	9.49 ± 0.30	9.67–12.73	11.34 ± 0.90
Na <sub>2</sub> O	1.17–4.93	1.54 ± 1.07	1.16–1.81	1.41 ± 0.21
K <sub>2</sub> O	2.58–2.79	2.72 ± 0.06	2.28–3.09	2.54 ± 0.24
P <sub>2</sub> O <sub>5</sub>	0.12–0.15	0.14 ± 0.01	0.12–0.14	0.13 ± 0.01
LOI	18.91–21.11	19.63 ± 0.73	16.15–20.67	18.08 ± 1.63
Trace elements (mg kg <sup>-1</sup> )				
		S1		E1
	Min-max	Mean	Min-max	Mean
As	8–12	10 ± 1	7–12	9 ± 2
Ba	272–320	291 ± 13	255–338	278 ± 24
Ce	47–73	63 ± 7	35–63	52 ± 9
Co	12–14	13 ± 1	10–13	11 ± 1
Cr	176–190	183 ± 4	132–146	139 ± 4
Cu	28–40	34 ± 3	15–23	18 ± 3
La	26–34	30 ± 2	19–29	23 ± 3
Nb	13–15	14 ± 1	13–14	14 ± 1
Ni	120–128	128 ± 3	71–95	80 ± 7
Pb	32–39	36 ± 3	18–29	22 ± 4
Rb	32–39	36 ± 3	88–120	100 ± 9
Sr	257–278	267 ± 8	295–415	339 ± 40
V	148–161	157 ± 4	138–159	151 ± 7
Y	24–26	25 ± 1	24–27	25 ± 1
Zn	114–138	129 ± 8	71–92	79 ± 7
Zr	100–118	104 ± 5	127–162	145 ± 12

## Appendix B

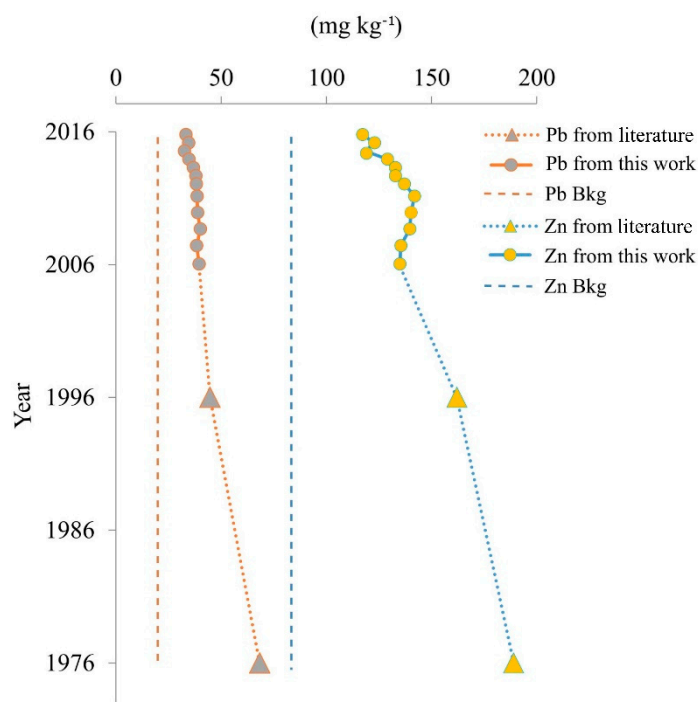


**Figure A1.** Pb and Zn historical concentration trends. Data from the literature [59,60] and this work (see Table 2).

## References

1. Heim, S.; Schwarzbauer, J. Pollution history revealed by sedimentary records: A review. *Environ. Chem. Lett.* **2013**, *11*, 255–270. [[CrossRef](#)]
2. Lima, A. Evaluation of geochemical background at regional and local scales by fractal filtering technique: Case studies in selected Italian areas. In *Environmental Geochemistry. Site Characterization, Data Analysis and Case Stories*; de Vivo, B., Belkin, H.E., Lima, A., Eds.; Elsevier: Amsterdam, The Netherlands, 2008; pp. 135–153.
3. Matteucci, G.; Rossini, P.; Guerzoni, S.; Arcangeli, A.; Fonti, P.; Langone, L. Recent evolution of sedimentary heavy metals in a coastal lagoon contaminated by industrial wastewaters (Pialassa Baiona, Ravenna, Italy). *Hydrobiologia* **2005**, *550*, 167–173. [[CrossRef](#)]
4. Pirrone, N.; Trombino, G.; Cinnirella, S.; Algieri, A.; Bendoricchio, G.; Palmeri, L. The Driver-Pressure-State-Impact-Response (DPSIR) approach for integrated catchment-coastal zone management: Preliminary application to the Po catchment Adriatic Sea coastal zone system. *Reg. Environ. Chang.* **2005**, *5*, 111–137. [[CrossRef](#)]
5. Abbiati, M.; Mistri, M.; Bartoli, M.; Ceccherelli, V.U.; Colangelo, M.A.; Ferrari, C.R.; Giordani, G.; Munari, C.; Nizzoli, D.; Ponti, M.; et al. Trade-off between conservation and exploitation of the transitional water ecosystems of the northern Adriatic Sea. *Chem. Ecol.* **2010**, *26*, 105–119. [[CrossRef](#)]
6. Zonta, R.; Cassin, D.; Pini, R.; Dominik, J. Assessment of heavy metal and as contamination in the surface sediments of Po delta lagoons (Italy). *Estuar. Coast. Shelf Sci.* **2019**, *225*, 106235. [[CrossRef](#)]
7. Romano, S.; Langone, L.; Frignani, M.; Albertazzi, S.; Focaccia, P.; Bellucci, L.G.; Ravaioli, M. Historical pattern and mass balance of trace metals in sediments of the northwestern Adriatic Sea Shelf. *Mar. Poll. Bull.* **2013**, *76*, 32–41. [[CrossRef](#)]
8. Lopes-Rocha, M.; Langone, L.; Miserocchi, S.; Giordano, P.; Guerra, R. Spatial patterns and temporal trends of trace metal mass budgets in the western Adriatic sediments (Mediterranean Sea). *Sci. Tot. Environ.* **2017**, *599–600*, 1022–1033. [[CrossRef](#)]



9. Poulain, P. Adriatic Sea surface circulation as derived from drifter data between 1990 and 1999. *J. Mar. Syst.* **2001**, *29*, 3–32. [[CrossRef](#)]
10. Lopes-Rocha, M.; Langone, L.; Miserocchi, S.; Giordano, P.; Guerra, R. Detecting long-term temporal trends in sediment-bound metals in the western Adriatic (Mediterranean Sea). *Mar. Poll. Bull.* **2017**, *124*, 270–285. [[CrossRef](#)]
11. Wang, X.H.; Pinardi, N. Modeling the dynamics of sediment transport and resuspension in the northern Adriatic Sea. *J. Geophys. Res. Space Phys.* **2002**, *107*, 3225. [[CrossRef](#)]
12. Davolio, S.; Stocchi, P.; Benetazzo, A.; Bohm, E.; Riminucci, F.; Ravaioli, M.; Li, X.; Carniel, S. Exceptional Bora outbreak in winter 2012: Validation and analysis of high-resolution atmospheric model simulations in the northern Adriatic area. *Dyn. Atmos. Oceans* **2015**, *71*, 1–20. [[CrossRef](#)]
13. Boldrin, A.; Langone, L.; Miserocchi, S.; Turchetto, M.; Aciri, F. Po River plume on the Adriatic continental shelf: Dispersion and sedimentation of dissolved and suspended matter during different river discharge rates. *Mar. Geol.* **2005**, *222*, 135–158. [[CrossRef](#)]
14. Milliman, J.D.; Syvitski, J.P.M. Geomorphic/tectonic control of sediment discharge to the ocean: The importance of small mountainous rivers. *J. Geol.* **1992**, *100*, 525–544. [[CrossRef](#)]
15. Frignani, M.; Langone, L.; Ravaioli, M.; Sorgente, D.; Alvisi, F.; Albertazzi, S. Fine-sediment mass balance in the western Adriatic continental shelf over a century time scale. *Mar. Geol.* **2005**, *222*, 113–133. [[CrossRef](#)]
16. Cattaneo, A.; Correggiari, A.; Langone, L.; Trincardi, F. The late-Holocene Gargano subaqueous delta, Adriatic shelf: Sediment pathways and supply fluctuations. *Mar. Geol.* **2003**, *193*, 61–91. [[CrossRef](#)]
17. Greggio, N.; Giambastiani, B.M.; Campo, B.; Dinelli, E.; Amorosi, A. Sediment composition, provenance, and Holocene paleoenvironmental evolution of the Southern Po River coastal plain (Italy). *Geol. J.* **2018**, *53*, 914–928. [[CrossRef](#)]
18. Montanari, A. Hydrology of the Po River: Looking for changing patterns in river discharge. *Hydrol. Earth Syst. Sci.* **2012**, *16*, 3739–3747. [[CrossRef](#)]
19. Ciavola, P.; Salemi, E.; Billi, P. *Sediment Supply and Morphological Evolution of a Small River Mouth (Fiumi Uniti, Ravenna, Italy): Should River Management be Storm-Driven*; Barazzutti, M., Marabini, F., Eds.; China-Italy Bilateral Symposium on the Coastal Zone and Continental Shelf Evolution Trend: Ravenna, Italy, 2010.
20. Pavanelli, D.; Cavazza, C.; Lavrić, S.; Toscano, A. The Long-Term Effects of Land Use and Climate Changes on the Hydro-Morphology of the Reno River Catchment (Northern Italy). *Water* **2019**, *11*, 1831. [[CrossRef](#)]
21. Maselli, V.; Pellegrini, C.; Del Bianco, F.; Mercorella, A.; Nones, M.; Crose, L.; Guerrero, M.; Nittrouer, J.A. River morphodynamic evolution under dam-induced backwater: An example from the Po River (Italy). *J. Sediment. Res.* **2018**, *88*, 1190–1204. [[CrossRef](#)]
22. Correggiari, A.; Cattaneo, A.; Carrà, D.; Penitenti, D.; Preti, M.; Trincardi, F. Offshore sand for beach restoration: North Adriatic shelf examples. *CIESM Workshop* **2002**, *18*, 79–82.
23. Matteucci, G.; Riccio, S.; Rossini, P.; Sisti, E.; Bernucci, M.E.; Pari, P.; Benedettini, M.; Stanley, C.C. Shoreline evolution trend connected to progressive construction of segmented defense structures (Rimini, North Adriatic Sea, Italy). *GeoActa* **2010**, *SI 3*, 135–141.
24. Di Matteo, L.; Dragoni, W.; Maccari, D.; Piacentini, S.M. Climate change, water supply and environmental problems of headwaters: The paradigmatic case of the Tiber, Savio and Marecchia rivers (Central Italy). *Sci. Total Environ.* **2017**, *598*, 733–748. [[CrossRef](#)] [[PubMed](#)]
25. Laghi, M.; Mollema, P.; Antonellini, M. The Influence of River Bottom Topography on Salt Water Encroachment along the Lamone River (Ravenna, Italy), and Implications for the Salinization of the Adjacent Coastal Aquifer. In Proceedings of the World Environmental and Water Resources Congress 2010: Challenges of Change, Providence, RI, USA, 16–20 May 2010; pp. 1124–1135.
26. Amorosi, A.; Sammartino, I. Influence of sediment provenance on background values of potentially toxic metals from near-surface sediments of Po coastal plain (Italy). *Intern. J. Earth Sci.* **2007**, *96*, 389–396. [[CrossRef](#)]
27. Amorosi, A.; Centineo, M.C.; Dinelli, E.; Lucchini, F.; Tateo, F. Geochemical and mineralogical variations as indicators of provenance changes in Late Quaternary deposits of SE Po Plain. *Sediment. Geol.* **2002**, *151*, 273–292. [[CrossRef](#)]
28. Amorosi, A. Chromium and nickel as indicators of source-to-sink sediment transfer in a Holocene alluvial and coastal system (Po Plain, Italy). *Sediment. Geol.* **2012**, *280*, 260–269. [[CrossRef](#)]

29. Ravaioli, M.; Alvisi, F.; Vitturi, L.M. Dolomite as a tracer for sediment transport and deposition on the northwestern Adriatic continental shelf (Adriatic Sea, Italy). *Cont. Shelf Res.* **2003**, *23*, 1359–1377. [[CrossRef](#)]
30. Dinelli, E.; Lucchini, F. Sediment supply to the Adriatic Sea basin from the Italian rivers: Geochemical features and environmental constraints. *Giorn. Geol.* **1999**, *61*, 121–132.
31. Marchesini, L.; Amorosi, A.; Cibin, U.; Zuffa, G.G.; Spadafora, E.; Preti, D. Sand composition and sedimentary evolution of a Late Quaternary depositional sequence, northwestern Adriatic Coast, Italy. *J. Sediment. Res.* **2000**, *70*, 829–838. [[CrossRef](#)]
32. Böhm, E.; Riminucci, F.; Bortoluzzi, G.; Colella, S.; Aciri, F.; Santoleri, R.; Ravaioli, M. Operational use of continuous surface fluorescence measurements offshore Rimini to validate satellite-derived chlorophyll observations. *J. Oper. Oceanogr.* **2016**, *9*, 167–175. [[CrossRef](#)]
33. Ravaioli, M.; Bergami, C.; Riminucci, F.; Langone, L.; Cardin, V.; Di Sarra, A.; Aracri, S.; Bastianini, M.; Bensi, M.; Bergamasco, A.; et al. The RITMARE Italian Fixed-Point Observatory Network (IFON) for marine environmental monitoring: A case study. *J. Oper. Oceanogr.* **2016**, *9*, 202–214. [[CrossRef](#)]
34. Capotondi, L.; Mancin, N.; Cesari, V.; Dinelli, E.; Ravaioli, M.; Riminucci, F. Recent agglutinated foraminifera from the North Adriatic Sea: What the agglutinated tests can tell. *Mar. Micropal.* **2019**, *147*, 25–42. [[CrossRef](#)]
35. Bastianini, M.; Riminucci, F.; Capotondi, L.; Barra, E.; Pasqual, S.; Casotti, R.; Trano, A.C.; Van Dijk, M.; Mauro, C.; Fabbro, C. Rapporto sulle attività oceanografiche, biologiche, geologiche e di manutenzione della stazione meda S1-GB svolte durante la campagna oceanografica LTER-ANOC16 (26–30 aprile 2016) con N/O Dallaporta nel Mare Adriatico settentrionale. *Rapp. Tec. CNR-ISMAR* **2017**, *145*, 1–27.
36. Bastianini, M.; Riminucci, F.; Pansera, M.; Coluccelli, A.; Casotti, R.; Dal Passo, E.; Dametto, L.; Van Dijk, M.; Russo, E.; Titocci, J.; et al. Rapporto sulle attività biologiche, oceanografiche, geologiche e di manutenzione della stazione Boa E1 svolte durante la campagna INTERNOS17 (14–21 marzo 2017) con N/O Minerva Uno nel Mare Adriatico centro-settentrionale. *Rapp. Tec. CNR-ISMAR* **2017**, *146*, 1–37.
37. Berner, R.A. *Principles of Chemical Sedimentology*; McGraw-Hill: New York, NY, USA, 1971; p. 240.
38. Albertazzi, S.; Bopp, R.F.; Frignani, M.; Merlin, O.H.; Vitturi, L.M.; Ravaioli, M.; Triulzi, C. Cs-137 as a tracer for processes of marine sedimentation in the vicinity of the Po River Delta (Northern Adriatic Sea). *Mem. Soc. Geol. Italy* **1984**, *27*, 447–459.
39. Frignani, M.; Langone, L.; Ravaioli, M.; Sticchi, A. Cronologia di sedimenti marini artificiali mediante spettrometria gamma. *IGM-CNR Tech. Rep.* **1991**, 24–32.
40. Covelli, S.; Fontolan, G. Application of a Normalization Procedure in Determining Regional Geochemical Baselines. *Environ. Geol.* **1997**, *30*, 34–45. [[CrossRef](#)]
41. Correggiari, A.; Bastianini, M.; Miserocchi, S. Caratterizzazione dei sedimenti dell'Alto Adriatico nell'ambito del Monitoraggio delle microalghe potenzialmente tossiche nelle aree marino-costiere del Veneto con una particolare attenzione a *Ostreopsis Ovata*. *Rapp. Tec. Cnr. Ismar. Bologna* **2016**, 1–30.
42. Morelli, G.; Gasparon, M.; Fierro, D.; Hu, W.P.; Zawadzki, A. Historical trends in trace metal and sediment accumulation in intertidal sediments of Moreton Bay, southeast Queensland, Australia. *Chem. Geol.* **2012**, *300–301*, 152–164. [[CrossRef](#)]
43. Frignani, M.; Sorgente, D.; Langone, L.; Albertazzi, S.; Ravaioli, M. Behavior of Chernobyl radiocesium in sediments of the Adriatic Sea off the Po River delta and the Emilia-Romagna coast. *J. Environ. Radioact.* **2004**, *71*, 299–312. [[CrossRef](#)]
44. Giani, M.; Boldrin, A.; Matteucci, G.; Frascari, F.; Gismondi, M.; Rabitti, S. Downward fluxes of particulate carbon, nitrogen, and phosphorus in the north-western Adriatic Sea. *Sci. Total Environ.* **2001**, *266*, 125–134. [[CrossRef](#)]
45. Alvisi, F. A simplified approach to evaluate sedimentary organic matter fluxes and accumulation on the NW Adriatic Shelf (Italy). *Chem. Ecol.* **2009**, *25*, 119–134. [[CrossRef](#)]
46. Rossi, A.; Roveri, N.; Albertazzi, S.; Focaccia, P.; Ravaioli, M. Elaborazione ed Interpretazione di dati Geochimici di Sedimenti Marini dell'area Adriatica Centro Settentrionale. Master's Thesis, University of Bologna, Bologna, Italy, 2011.
47. Giordani, P.; Hammond, D.E.; Berelson, W.M.; Montanari, G.; Poletti, R.; Milandri, A.; Rabbi, E. Benthic fluxes and nutrient budgets for sediments in the Northern Adriatic Sea: Burial and recycling efficiencies. *Mar. Coas. Eutroph.* **1992**, 251–275. [[CrossRef](#)]

48. Picone, S.; Alvisi, F.; Dinelli, E.; Morigi, C.; Negri, A.; Ravaioli, M.; Vaccaro, C. New insights on late Quaternary palaeogeographic setting in the Northern Adriatic Sea (Italy). *J. Quat. Sci.* **2008**, *23*, 489–501. [[CrossRef](#)]
49. Spagnoli, F.; Dinelli, E.; Giordano, P.; Marcaccio, M.; Zaffagnini, F.; Frascari, F. Sedimentological, biogeochemical and mineralogical facies of Northern and Central Western Adriatic Sea. *J. Mar. Syst.* **2014**, *139*, 183–203. [[CrossRef](#)]
50. Colantoni, P.; Gallignani, P.; Lenaz, R. Late Pleistocene and Holocene evolution of the North Adriatic continental shelf (Italy). *Mar. Geol.* **1979**, *33*, 41–50. [[CrossRef](#)]
51. Amorosi, A.; Guermandi, M.; Marchi, N.; Sammartino, I. Fingerprinting sedimentary and soil units by their natural metal contents: A new approach to assess metal contamination. *Sci. Total Environ.* **2014**, *500–501*, 361–372. [[CrossRef](#)]
52. APAT; ICRAM. *Manuale per la Movimentazione di Sedimenti Marini*; Corsini, S., Onorati, F., Pellegrini, D., Eds.; Ministero per l'ambiente e la tutela del territorio e del mare: Rome, Italy, 2006; p. 72.
53. Price, B.N.; Mowbray, S.; Giordani, P. *Sedimentation and Heavy Metal Input Changes of the Northwest Adriatic Shelf: A Consequence of Anthropogenic Activity*; Atti 108 Congresso AIOL.: Alassio, Italy, 1994; pp. 23–33.
54. Maselli, V.; Trincardi, F. Man made deltas. *Sci. Rep.* **2013**, *3*, 1926. [[CrossRef](#)]
55. Stefani, M.; Vincenzi, S. The interplay of eustasy, climate and human activity in the late Quaternary depositional evolution and sedimentary architecture of the Po Delta system. *Mar. Geol.* **2005**, *222*, 19–48. [[CrossRef](#)]
56. Trincardi, F.; Amorosi, A.; Bosman, A.; Correggiari, A.; Madricardo, F.; Pellegrini, C. Ephemeral rollover points and clinotherm evolution in the modern Po Delta based on repeated bathymetric surveys. *Basin Res.* **2020**, *32*, 402–418. [[CrossRef](#)]
57. Billi, P.; Salemi, E. Misura del Trasporto Solido del Fiume Reno. In *2° Giornata di Studio—Il Monitoraggio Idrotorbidimetrico dei Corsi D'acqua per la Stima dei Processi Erosivi e il Bilancio dei solidi Sospesi*; University of Ferrara: Ferrara, Italy, 2004.
58. Lee, C.M.; Askari, F.; Book, J.; Carniel, S.; Cushman-Roisin, B.; Dorman, C.; Kuzmic, M. Northern Adriatic response to a wintertime bora wind event. *Eos Trans. Amer. Geoph. Union* **2005**, *86*, 157–165. [[CrossRef](#)]
59. Ianni, C.; Magi, E.; Rivaro, P.; Ruggieri, N. Trace metals in Adriatic coastal sediments: Distribution and speciation pattern. *Toxic. Environ. Chem.* **2000**, *78*, 73–92. [[CrossRef](#)]
60. Frascari, F.; Frignani, M.; Giordani, P.; Guerzoni, S.; Ravaioli, M. Sedimentological and geochemical behavior of heavy metals in the area near the Po river delta. *Mem. Soc. Geol. Italy* **1984**, *27*, 469–481.
61. Annibaldi, A.; Truzzi, C.; Illuminati, S.; Scarponi, G. Recent sudden decrease of lead in Adriatic coastal seawater during the years 2000–2004 in parallel with the phasing out of leaded gasoline in Italy. *Mar. Chem.* **2009**, *113*, 238–249. [[CrossRef](#)]
62. Guerzoni, S.; Frignani, M.; Giordani, P.; Frascari, F. Heavy metals in sediments from different environments of a Northern Adriatic Sea area, Italy. *Environ. Geol. Water Sci.* **1984**, *6*, 111–119. [[CrossRef](#)]
63. Giani, M.; Gabellini, M.; Pellegrini, D.; Costantin, S.; Beccaloni, E.; Giordano, R. Concentration and partitioning of Hg, Cr and Pb in sediments of dredge and disposal sites of the northern Adriatic Sea. *Sci. Total Environ.* **1994**, *158*, 97–112. [[CrossRef](#)]

